

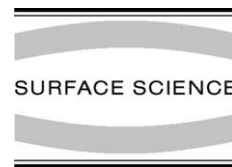


ELSEVIER

Available online at www.sciencedirect.com

SCIENCE @ DIRECT®

Surface Science 531 (2003) 359–367



www.elsevier.com/locate/susc

Initial oxidation kinetics of copper (1 1 0) film investigated by in situ UHV-TEM

Guangwen Zhou^{*}, Judith C. Yang

Department of Materials Science and Engineering, University of Pittsburgh, 848 Benedum Hall, Pittsburgh, PA 15261, USA

Received 21 October 2002; accepted for publication 19 March 2003

Abstract

Previous studies of the initial stage of oxidation on clean single crystal of Cu(1 0 0) have been extended to the case of the Cu(1 1 0) surface. The dynamic observation of the nucleation and growth of Cu oxide by means of in situ ultra high vacuum transmission electron microscopy (UHV-TEM) shows a highly enhanced oxidation rate on Cu(1 1 0) surface as compared to Cu(1 0 0). The kinetic data on the nucleation and growth of the three-dimensional oxide islands agree well with our heteroepitaxial model of surface diffusion of oxygen.

© 2003 Elsevier Science B.V. All rights reserved.

Keywords: Copper; Oxidation; Electron microscopy; Nucleation; Surface diffusion

1. Introduction

Classical theories of oxidation, such as Cabrera–Mott, [1] have proved to be highly successful in predicting oxidation behavior of metals, but these models are focused on the growth of an oxide layer, and assumes uniform film growth. Due to the development of well-controlled experiments and the increased experimental capabilities in resolution and cleanliness, it is known that early stages of oxidation involve nucleation and growth of metal oxide islands [2–6]. However, there is still a wide gap between information provided by surface science methods (adsorption of up to ~ 1 ML of oxygen) and that provided by bulk oxidation

studies (oxide layer of \sim few microns or thicker). The initial state of a metal surface, such as surface impurities and surface morphology, may greatly influence the oxide nucleation, growth and hence the oxide film structure. Hence, we have chosen to study the initial stage of oxidation by in situ ultra high vacuum transmission electron microscopy (UHV-TEM), which can bridge the gap between monolayer and bulk growth and where the UHV environment provides excellent control of surface conditions. By means of in situ UHV-TEM we can study quantitatively the dynamic aspect of the initial stage of oxidation, for example the oxide nucleation and growth.

Oxygen reaction with Cu surfaces is considered to be a model system for the oxidation of metal surfaces and has consequently been studied extensively [7–11]. We had previously reported our investigations of the kinetics of initial stages of Cu(1 0 0) oxidation using in situ UHV-TEM [3,

^{*} Corresponding author. Tel.: +1-412-6249753; fax: +1-412-6248069.

E-mail address: guzstl@pitt.edu (G. Zhou).

12–15]. We have demonstrated that oxygen surface diffusion is the dominant mechanism for the oxide formation during the initial oxidation in dry oxygen atmosphere and shown that heteroepitaxial concepts describe surprisingly well the nucleation, and growth to coalescence of Cu_2O island on $\text{Cu}(001)$. This paper focuses on the oxidation of $\text{Cu}(110)$. Although the rate of oxidation on $\text{Cu}(110)$ is faster than $\text{Cu}(100)$, the same models of oxygen surface diffusion agree exceptionally with the experimental data.

Gwathmey and co-workers [8,16] have demonstrated that the oxidation phenomena observed on copper vary with crystal orientation. Investigations by Benard and co-workers [17,18] showed that the rates of oxidation were different for different crystal orientations. In the present work we present a systematic investigation of the kinetics of the initial oxidation on $\text{Cu}(110)$ surface by in situ UHV-TEM. Interestingly, the apparent discrepancy between Gwathmey et al.'s results of $\text{Cu}(110)$ having oxidation rate and the results presented here can be explained by heteroepitaxial concepts coalescence. We have examined the dependence of island density on oxidation time, saturation island density on oxidation temperature, and island growth as a function of oxidation time. The results presented here for the $\text{Cu}(110)$ surface reveal the similarities and differences observed for $\text{Cu}(100)$ and $\text{Cu}(110)$, and demonstrate the generality of the oxygen surface diffusion model originally developed to describe the results observed on the $\text{Cu}(100)$ surface. Before presenting the results for $\text{Cu}(110)$ surface, we will briefly discuss the oxygen surface diffusion model for oxide nucleation and growth in the following section.

2. Oxygen surface diffusion model

2.1. Nucleation

Oxygen gas molecules impinge on the metal surface and dissociate. The chemisorbed oxygen creates a Cu-O surface reconstruction. It is probable that the further impinging oxygen molecules dissociate into oxygen atoms, and then diffuse across the O-chemisorbed surface, where they may

be lost to re-evaporation, form new oxide nuclei, or be captured by an existing nuclei. Regardless of the details of the intermediate steps, the density of these stable nuclei is expected to increase with time, reaches a saturation level, N_s , and then decreases as the discrete nuclei impinge on each other and coalesce. One consequence of oxygen surface diffusion being the mechanism for nucleation is there is a saturation island density, $1/L_d^2$, where L_d^2 is the area of the “zone of oxygen capture” around each Cu_2O islands. An oxygen concentration gradient exists across this zone such that oxygen that lands within this zone shall diffuse to the Cu_2O islands; hence, the oxide islands act as oxygen sinks.

Assuming oxygen surface diffusion is the dominant transport mechanism for the nucleation of copper oxides, then the probability of an oxide nucleation event is proportional to the fraction of the available surface area outside these “zones of oxygen capture” and the oxide nucleus density can be determined to be [13]

$$N = \frac{1}{L_d^2} (1 - e^{-kL_d^2 t}), \quad (1)$$

where L_d^2 is the area of the zone of oxygen capture, $1/L_d^2$ is the saturation island density, L_d is much larger than the diameter of the oxide island, k is the initial nucleation rate, which depends on the probability for Cu and O to form Cu_2O , and t is the oxidation time.

Because of higher mobility of oxygen at higher temperatures, the attachment to existing island is more favorable than the nucleation of new nuclei. Hence, it is reasonable to expect many small islands are formed at low temperatures, whereas for high temperatures less island density but larger average island size is observed. Therefore, the saturation island density dependence on temperature could follow an Arrhenius relationship,

$$N_s \sim e^{E_a/kT}, \quad (2)$$

where k is the Boltzmann constant, T is the oxidation temperature. This activation energy, E_a , of the nucleation depends on the energies of nucleation, absorption and/or desorption [19] and not necessarily on the oxygen surface diffusion energy only. By measuring the island density at different temperatures, then the activation energy, E_a , for this surface-limited nucleation process can be determined.

2.2. Growth

Orr, [20] followed by Holloway and Hudson [21], has developed an oxidation model based on the assumption that oxygen surface diffusion should play a major role in the initial growth of the metal oxide. They assumed that the oxide islands grew on the metal surface, i.e. two-dimensional (2-D) and obtained a parabolic growth rate law if oxygen surface diffusion and impingement on the island's perimeter is the dominant transport mechanism.

The formation of oxide is accompanied the conversion of copper atoms from the substrate to Cu_2O islands, therefore, the oxide islands should grow three-dimensionally (3-D) into the substrate. We have extended Orr's model to incorporate the 3-D growth. Following the derivation of Orr, oxygen surface diffusion to the perimeter of an oxide island creates a growth rate [21],

$$\frac{dN(t)}{dt} = 2\pi r J_s, \quad (3)$$

where $N(t)$ is the number of oxygen atoms in Cu_2O island at time t , r is the radius of the circular profile of an island, J_s is the actual flux of oxygen incorporated into Cu_2O island. The concentration of oxygen molecules at the edge of the Cu_2O island is C_i , by assuming steady state growth of Cu_2O island, the C_i can be obtained to be

$$C_i = \frac{DC_o}{K_s L_d + D}, \quad (4)$$

where L_d is the radius of oxygen capture zone of Cu_2O islands, C_o is surface concentration of oxygen far away from Cu_2O islands, D is the surface diffusion coefficient of oxygen, K_s is the sticking coefficient of oxygen to in Cu_2O island. For 2-D lateral growth of a disk-shaped island, with thickness a , then by solving the above differential equation, Eq. (3), the cross-sectional area increases parabolically with respect to time [21]. Following a similar analysis for 3-D growth of a spherical island, then the cross-sectional area, A , of the oxide island, is

$$A(t) = \frac{\pi\Omega K_s DC_o}{D + L_d K_s} (t - t_0), \quad (5)$$

where Ω is the volume occupied by one O atom in Cu_2O . The power law dependence, t^2 for 2-D and t for 3-D, is independent of the shape of the island.

3. Experiment

The microscope used in this work was a modified JEOL 200CX [22]. A UHV chamber was attached to the middle of the column, where the base pressure was less than 10^{-8} Torr without the use of the cryoshroud. The cryoshroud inside the microscope column can reduce the base pressure to approximately 10^{-9} Torr when filled with liquid helium. The microscope was operated at 100 keV in order to minimize irradiated effects. A leak valve attached to the column of the microscope permits the introduction of gases directly into the microscope. The specially designed sample holder allows for resistive heating at temperatures between room temperature and 1000 °C. A 5- μm objective aperture was used in order to enhance the contrast of the dark field images. Single crystal 99.999% pure Cu(1 1 0) films were grown on irradiated (1 1 0)NaCl in an UHV e-beam evaporator system, where the base pressure was 10^{-10} Torr. 700 Å thick Cu(1 1 0) films were examined so that the films were thin enough to be examined by TEM. The copper film was removed from the substrate by floatation in deionized water, washed and mounted on a specially prepared Si mount. The native Cu oxide was removed inside the TEM by annealing the Cu films in methanol vapor at a pressure of 5×10^{-5} Torr and 350 °C, which reduces the copper oxides to copper [23]. Scientific grade oxygen gas of 99.999% purity can be admitted into the column of the microscope through the leak valve at a partial pressure between 5×10^{-5} and 760 Torr.

4. Results

4.1. Nucleation of oxide islands

The in situ observation of the island nucleation events as function of time provides significant insights into the oxidation kinetics. Fig. 1(a) is a dark field TEM image after the copper film has been cleaned with methanol. No oxide islands are visible in this region. Fig. 1(b) and (c) show the corresponding dark field images at the same area as shown in Fig. 1(a) of the copper film at successive 10 min time increments after oxygen was

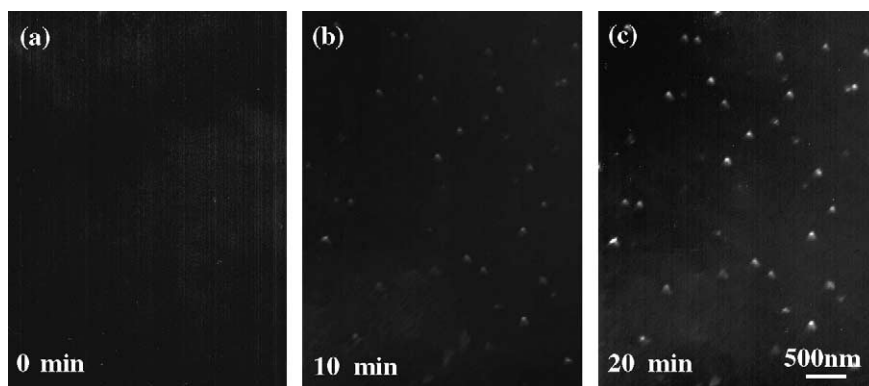


Fig. 1. In situ bright field TEM images taken as a function of oxidation time: (a) 0 min, (b) 10 min, (c) 20 min at constant oxygen partial pressure of 5×10^{-4} and temperature of 350 °C.

leaked into the column of the microscope. The partial pressure of oxygen was 5×10^{-4} Torr and the temperature of the copper film was held at 350 °C. After the introduction of oxygen gas, the nuclei appear after an incubation period of several minutes. After the oxidation of about 22 min, no new islands formed, and the islands reached the saturation density of the nuclei. The selected area electron diffraction pattern of the Cu_2O island and underlying $\text{Cu}(110)$ substrate revealed that the oxide island is epitaxial with the underlying Cu film, i.e. $(1\bar{1}0)\text{Cu} // (1\bar{1}0)\text{Cu}_2\text{O}$ and $(001)\text{Cu} // (001)\text{Cu}_2\text{O}$. A similar epitaxial relationship was noted for $\text{Cu}(100)$, where $(001)\text{Cu} // (001)\text{Cu}_2\text{O}$ and $(010)\text{Cu} // (010)\text{Cu}_2\text{O}$ [24].

To measure quantitatively the number density and cross-sectional area of the oxide islands, the negatives were digitized with a Leafscan™ 45. The software packages Digital Micrograph™ and NIH Image™ were used to determine the number density and the cross-section as a function of oxidation time. Fig. 2 shows the experimental data and theoretical fit to Eq. (1), where the ranges of the error bars are based on the measured oxide island density obtained from several experimental runs and different regions on the Cu surface. A good match is noted where the fit parameters, $k = 1.7432$, and $L_d = 0.3331$. Hence the initial nucleation rate, k , is $1.7432 \mu\text{m}^{-2} \text{min}^{-1}$, and the saturation island density, $1/L_d^2$, is $9.01159 \mu\text{m}^{-2}$. In comparison, our previous work on $\text{Cu}(100)$ at the same oxidation conditions of 350 °C and oxygen

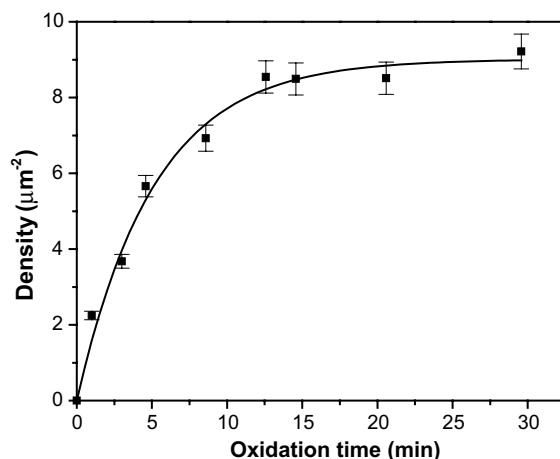


Fig. 2. Cu_2O island density as a function of oxidation time at constant oxygen partial pressure of 5×10^{-4} and temperature of 350 °C.

pressure of 5×10^{-4} Torr revealed that the oxide islands reached saturation density of nuclei, $0.8 \mu\text{m}^{-2}$, after 25 min oxidation. The radius, L_d , of active zone of oxygen capture around each island was determined to be $1.09 \mu\text{m}$ long before the islands impinge on each other. The initial nucleation rate, k , is $0.17 \mu\text{m}^{-2} \text{min}^{-1}$.

We measured the saturation density of the nuclei as a function of oxidation temperature, from 300 to 450 °C, at constant oxygen pressure of 5×10^{-4} Torr. Fig. 3 shows the saturation density of nuclei versus inverse oxidation temperature, where the activation energy, E_a , which is equal to

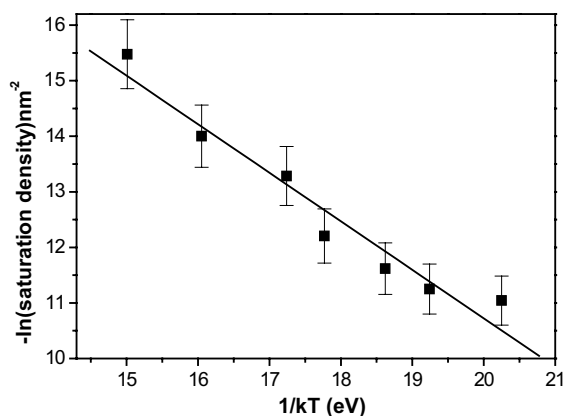


Fig. 3. Cu_2O saturation island density versus inverse temperature. The absolute value of the slope is the E_a for the surface-limited process.

the slope, was determined to be 1.1 ± 0.2 eV. In comparison, the activation energy, E_a , for Cu(100) was measured to be 1.4 ± 0.2 eV [13].

4.2. Growth

The evolution of cross-section area of the islands is recorded in situ, and a sequence of images focusing on the growth of individual islands is shown in Fig. 4, where the Cu(110) film was oxidized at 5×10^{-4} Torr and 450°C . About a couple of minutes after the introduction of oxygen gas, Cu_2O islands were observed to nucleate rapidly followed by growth of these islands. After the

initial nucleation of the oxide islands, ~ 5 min, the saturation density of the island nuclei was reached and no new nucleation event was observed, which is much faster than the oxidation at 350°C , where the saturation is reached after 22 min oxidation.

Fig. 5 is the comparison of the experimental data of the oxide volume to this surface diffusion model by using 3-D growth of oxide island, Eq. (5), where the ranges of the error bars are also based on the measured oxide island cross-sectional area obtained from several experimental runs and different regions on the Cu surface. The kinetic data on the evolution of cross-section area of the

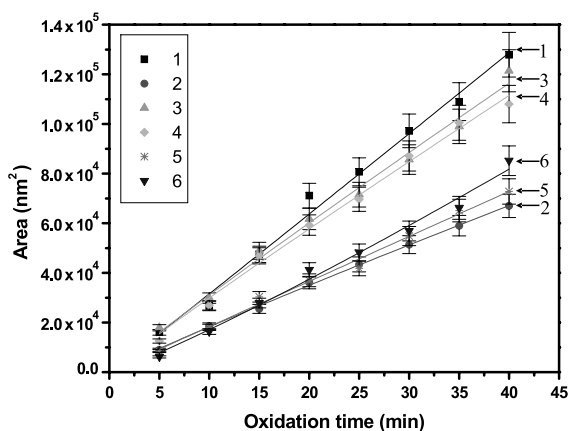


Fig. 5. Comparison of the experimental data and the theoretical function for the surface diffusion for the 3-D growth of Cu_2O islands.

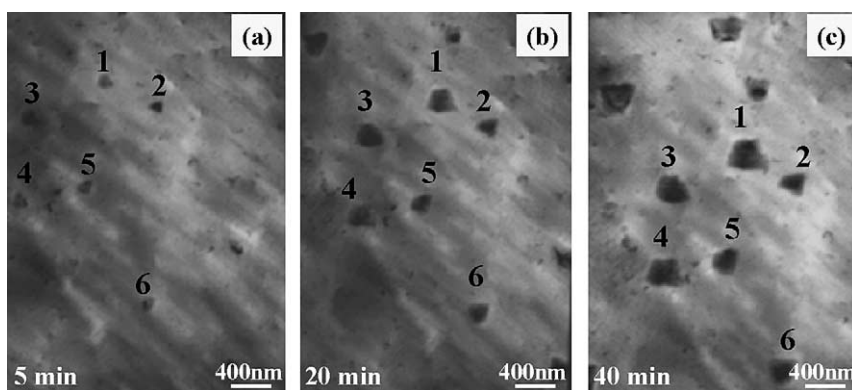


Fig. 4. In situ bright field TEM image showing the growth of Cu_2O islands. Note that there is a saturation of the island nuclei.

islands agree well with the model of surface diffusion of oxygen. Therefore, the excellent agreement of evolution of cross-section area of the islands with the kinetic model validates that the growth of the 3-D Cu₂O islands occurs by oxygen surface diffusion and impingement on the oxide perimeter.

5. Discussion

The comparison of the nucleation and growth behavior of Cu(1 10) with that of Cu(100) at the same oxidation temperature (350 °C) and oxygen pressure (5×10^{-4} Torr) revealed that the same surface diffusion models, originally developed to describe Cu(100) oxidation, explains the experimental data on Cu(1 10) quite well and demonstrates a greater generality of this oxygen surface diffusion model.

Since the initial oxidation stages are surface processes, it is reasonable to expect that the crystallographic orientation of the underlying metal will have a major effect on the nucleation behavior, growth rate and the orientation of the oxide film. Table 1 summarizes the values of the fit parameters for Cu(100) and Cu(1 10) oxidation. Differences in the rate, oxide island shapes, and fit parameters to the surface models were noted between Cu(100) and Cu(1 10). Specifically, The initial nucleation rate on Cu(1 10) is much faster than Cu(100). The saturation density on Cu(1 10) surface is 11 times larger than that on Cu(100), although the oxide islands reached their saturation density after similar oxidation time for the two orientations. Hence, the active zone of oxygen

capture around each island on Cu(1 10) is much smaller than that on Cu(100). The activation energy, E_a , for the nucleation process on Cu(1 10), was measured to be 1.1 ± 0.2 eV, which is also smaller than that on Cu(100) surface, 1.4 ± 0.2 eV.

The oxygen surface model assumes homogeneous nucleation, not heterogeneous nucleation. One particularly interesting question is the role of defects, such as dislocation and steps in the initial oxide nucleation. In the oxidation of Cu(100), no preferential nucleation sites at dislocations or surface steps were observed [13,25]. Similar as in the oxidation of Cu(1 10), repeated oxidation, reduction, followed by oxidation experiments were performed, but no nuclei appeared at the same positions. Furthermore, the oxide island density was observed to decrease with increasing temperature, following as Arrhenius dependence, indicates that nucleation was homogeneous. If the nucleation mechanism was heterogeneous, then it would be reasonable to expect similar island density at different temperatures, which was not observed.

Since we are interested in the initial oxidation mechanisms, then it is essential to isolate the effect of the electron beam on the oxidation kinetics. In order to minimize the possible radiation damage, the TEM was operated only at 100 keV. Careful oxidation experiments with and without the electron beam irradiation were conducted. Qualitatively, the structural changes appeared similar as with the electron beam on. However, the effect of the electron beam was to reduce the reaction rate slightly, but the saturation density of the oxide islands was observed in both cases, indicative of a surface diffusion limited nucleation mechanism. This is again similar to the Cu(100) oxidation [13,25].

Both Cu(100) and Cu(1 10) oxidation were well-described by the oxygen surface diffusion—homogeneous nucleation model. The differences in the fit parameters obtained from the oxygen surface diffusion should be due to the crystallography effects. To explain these differences, we consider the effects of kinetics and energetics on both surfaces. The nucleation and growth of oxide islands are nonequilibrium processes depending on both

Table 1
Comparison of fit parameters of Cu(1 10) and Cu(100) oxidation

Parameters	Cu(100)	Cu(1 10)
Initial oxidation rate ($\mu\text{m}^{-2} \text{min}^{-1}$), k	0.17	1.7432
Saturation island density (μm^{-2}), $1/L_d^2$	0.83	9.01
Radius of oxygen capture zone (μm), L_d	1.09	0.33
Overall activation of nucleation (eV), E_a	1.4 ± 0.2	1.1 ± 0.2

the energetics, such as surface energies of the system, and the kinetics, in particular, on the diffusion process.

5.1. Kinetics considerations

It should be noted that the diffusion of oxygen is on the reconstructed Cu surface. Previous investigators have elegantly demonstrated that Cu(100) and Cu(110) surfaces are unreconstructed, and then transform into “missing-row” or “adding-row” reconstruction when exposed to oxygen [26–30]. Oxygen chemisorption on Cu surface is the first step for the oxidation. We speculate that the impinging oxygen molecules dissociate into oxygen atoms, and the dissociated oxygen is adsorbed at the Cu surface to form Cu–O bonds and create a surface reconstruction. After reconstruction, the oxygen atoms diffuse on this reconstructed surface, and nucleation occurs on the reconstructed Cu–O surface. Future arriving oxygen can either nucleate new oxide islands by reacting with copper atoms or attach to an existing islands, causing growth. Therefore, the surface diffusion coefficient of oxygen determines the outcome of the competition between nucleation and growth, and, hence, determines the number density of stable islands. Qualitatively a larger diffusion coefficient for oxygen should yield a lower number density of stable islands. Since the path length of oxygen surface diffusion depends on the atomic structure of the substrate plane, different nucleation behavior of Cu₂O islands is therefore expected for different orientations of the Cu. The Cu(100) has a more close-packed structure, and is smoother than the corrugated Cu(110) surface. Similarly, the reconstructed $(\sqrt{2} \times 2\sqrt{2})R45^\circ$ O–Cu(100) surface has a more compact oxygen chemisorption than (2×1) O–Cu(110) surface which has a corrugated structure, as shown in Fig. 6. Therefore, it is reasonable to expect the activation barrier of surface diffusion of the dissociated oxygen will be higher on the Cu(110) surface, and thus have a shorter path length. The shorter diffusion path length will give rise to a smaller capture zone of oxygen and create a higher number density of oxide nuclei. As a result, the nucleation process is dominated in the oxidation of Cu(110). This is

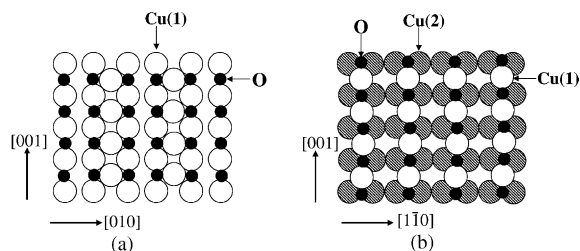


Fig. 6. Schematic diagram of the reconstructed $(\sqrt{2} \times 2\sqrt{2})R45^\circ$ O–Cu(100) surface (a), and (2×1) O–Cu(110) surface (b) due to oxygen chemisorption. Filled circles: O atoms; open circles: top layer Cu atoms; shaded circles: second layer Cu atoms.

confirmed by our results where the active zone of oxygen capture around each island on Cu(110) is $0.3331 \mu\text{m}$, which is significantly smaller than that on Cu(100), $1.09 \mu\text{m}$.

5.2. Energetics considerations

In order to form oxide islands on the surface, the system should overcome an activation barrier whose height is given by the work of formation of the critical nuclei. The number of critical nuclei per unit area is

$$N_{r^*} = N_0 \exp\left(-\frac{\Delta F^*}{kT}\right), \quad (6)$$

where r^* is the radius of the critical nucleus, N_0 is the number of adsorption sites per unit area of substrate surface, ΔF^* is the free energy of formation of the critical nucleus, and k and T have their usual meaning. The main contributions to ΔF^* are volume energy, surface/interfacial energy, and interfacial strain energy, due to elastic relaxations, during the formation and growth of the oxide nuclei.

The volume energy should be same for the oxide islands formed on Cu(100) and Cu(110) surfaces since only Cu₂O was observed to form. The differences in surface energies of substrates play an important role in the nucleation behavior. The surface with higher surface energy will be easier for island nucleation. The surface energy of Cu(100) is 1280 mJ/m^2 , which is lower than the Cu(110), 1400 mJ/m^2 [31]. If all other interface and surface energies were equal, then, it would be

expected that Cu(110) surface will be less stable under the oxidizing atmosphere and the nucleation of oxide islands will be facilitated, leading a higher nuclei density of oxide and smaller overall activation energy for the nucleation of the oxide islands as determined by our measurements. As yet, the surface energies of Cu₂O and the interfacial energies between Cu₂O/Cu(100) and Cu₂O/Cu(110) are unreported. The interfacial strain energy could depend on orientation since it is a function of the Poisson ratio (ν) and shear modulus (μ) of the substrate, as well as oxide island bulk stress (σ_b) [15,32], and is also not known in Cu₂O/Cu system. Hence, determination of the surface energies and metal–oxide interfacial energies, such as by theoretical modeling, are critical to fundamentally quantitative understanding of oxidation.

5.3. Comparison to previous research on Cu oxidation

Previous research by Lawless and Gwathmey [7] in the oxidation of a spherical single crystal of Cu with its multitude of surface orientation demonstrated the anisotropy of the oxidation rate on different faces. Fig. 7 is a reproduction of their experimental data on Cu(100) and Cu(110) in which Cu(100) has a much faster oxidation rate than Cu(110). Our early work on Cu(100) and present Cu(110) work have demonstrated that the

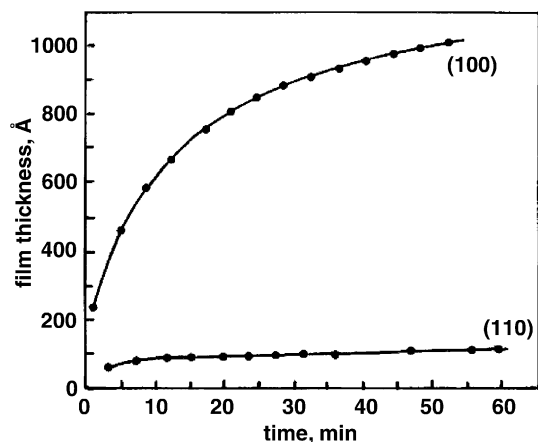


Fig. 7. Oxidation kinetics of copper single crystals at 523 K and 1 atm of oxygen from [7].

oxide film nucleates and grows as oxide islands, not as a uniform layer, even at atmospheric pressure [3]. During the progressive exposure of the Cu surface to oxygen, several stages are identifiable. The first stage is the dissociation and chemisorption of oxygen on the Cu surface. With the further exposure to oxygen, the epitaxial nuclei of oxide islands appear on the reconstructed surface after an incubation period. The islands will grow and coalesce with the continued exposure to oxygen. In these stages oxygen transport is dominated by surface and interface diffusion. Once coalescence has completed, then there should be a sudden reduction in the growth rate of the oxide, due the change of oxidation of the surface to diffusion through an oxide layer. Therefore, the self-limiting oxidation is due to the coalescence of islands, which switches off the surface diffusion route and requires much slower bulk diffusion for further oxidation.

As discussed in the preceding, Cu(110) shows a faster nucleation rate of oxide than Cu(100) in the initial stage of oxidation, and the oxidation on Cu(110) surface results in a higher number density of oxide nuclei under the same oxidation conditions. Therefore, there is a faster coalescence of oxide islands on Cu(110) than that on Cu(100). In the oxidation of Cu(100), it takes a longer oxidation time for the coalescence of oxide islands due to less number density of oxide nuclei. As a result, Cu(100) shows a faster oxidation rate than Cu(110) at the later stage of oxidation as confirmed by Lawless and Gwathmey's work [7]. Surprisingly, orientations that form a higher density oxide nuclei and have a faster initial oxidation rate, may have a slower long-term growth rate due to the rapid coalescence of the oxide which switches the oxide growth mechanism from surface diffusion to the slower diffusion through an oxide scale.

6. Conclusions

Cu(110) surface shows a highly enhanced oxidation rate than Cu(100) in the initial stage of oxidation. The oxide islands grow three-dimensionally, and surface diffusion of oxygen is the dominant transport mechanism for the oxide nu-

cleation and growth. The faster oxidation rate is explained by the smaller path length of surface diffusion of oxygen on Cu(1 1 0) and larger surface energy of Cu(1 1 0).

Acknowledgements

This research project is funded by the National Science Foundation (#9902863), Department of Energy–Basic Energy Science and a National Association of Corrosion Engineers seed grant. The experiments were performed at the Materials Research Laboratory, University of Illinois at Urbana-Champaign, which is supported by the US Department of Energy (#DEFG02-96-ER45439). The authors kindly thank I. Petrov, R. Twisten, M. Marshall, K. Colravy, and N. Finnegan for their help.

References

- [1] N. Cabrera, N.F. Mott, *Rep. Prog. Phys.* 12 (1948) 163.
- [2] K.R. Lawless, *Rep. Prog. Phys.* 37 (1973) 231.
- [3] J.C. Yang, B. Kolasa, J.M. Gibson, M. Yeadon, *Appl. Phys. Lett.* 73 (1998) 2481.
- [4] S. Aggarwal, A.P. Monga, S.R. Perusse, R. Ramesh, V. Ballarotto, E.D. Williams, B.R. Chalamala, Y. Wei, R.H. Reuss, *Science* 287 (2000) 2235.
- [5] S. Aggarwal, S.B. Ogale, C.S. Ganpule, S.R. Shinde, V.A. Novikov, A.P. Monga, M.R. Burr, R. Ramesh, V. Ballarotto, E.D. Williams, *Appl. Phys. Lett.* 78 (2001) 1442.
- [6] S.R. Shinde, A.S. Ogale, S.B. Ogale, S. Aggarwal, V. Novikov, E.D. Williams, R. Ramesh, *Phys. Rev. B* 64 (2001) 5408.
- [7] K.R. Lawless, A.T. Gwathmey, *Acta Metall.* 4 (1956) 153.
- [8] F. Young, J. Cathcart, A. Gwathmey, *Acta Metall.* 4 (1956) 145.
- [9] R.H. Milne, A. Howie, *Philos. Mag. A* 49 (1984) 665.
- [10] A. Roennquist, H. Fischmeister, *J. Inst. Met.* 89 (1960–1961) 65.
- [11] K. Heinemann, D.B. Rao, D.L. Douglas, *Oxid. Met.* 9 (1975) 379.
- [12] J.C. Yang, M. Yeadon, B. Kolasa, J.M. Gibson, *Appl. Phys. Lett.* 70 (1997) 3522.
- [13] J.C. Yang, M. Yeadon, B. Kolasa, J.M. Gibson, *Scr. Mater.* 38 (1998) 1237.
- [14] J.C. Yang, D. Evan, L. Tropia, *Appl. Phys. Lett.* 81 (2002) 241.
- [15] G.W. Zhou, J.C. Yang, *Phys. Rev. Lett.* 89 (2002) 106101.
- [16] A.T. Gwathmey, K.R. Lawless, in: H.C. Gatos (Ed.), *The Surface Chemistry of Metals and Semiconductors*, John Wiley, New York, 1960, p. 483.
- [17] J. Bardolle, J. Benard, *Rev. Met.* 49 (1952) 613.
- [18] J. Benard, F. Gronlund Jr., Oudar, M. Duret, *Z. Elektrochem. Ber. Bunsenges Physik, Chem.* 63 (1959) 799.
- [19] J.A. Venables, G.D.T. Spiller, M. Hanbuecken, *Rep. Prog. Phys.* 47 (1984) 399.
- [20] W.H. Orr, Ph.D thesis, Cornell University, 1962.
- [21] P.H. Holloway, J.B. Hudson, *Surf. Sci.* 43 (1974) 123.
- [22] M.L. McDonald, J.M. Gibson, F.C. Unterwald, *Rev. Sci. Instrum.* 60 (1989) 700.
- [23] S.M. Francis, F.M. Leibsle, S. Haq, N. Xiang, M. Bowker, *Surf. Sci.* 315 (1994) 284.
- [24] J.C. Yang, M.D. Bharadwaj, G.W. Zhou, L. Tropia, *Microsc. Microanal.* 7 (2001) 486.
- [25] J.C. Yang, M. Yeadon, B. Kolasa, J.M. Gibson, *J. Electrochem. Soc.* 146 (1999) 2103.
- [26] J.G. Tobin, L.E. Klebanoff, D.H. Rosenblatt, R.F. Davis, *Phys. Rev. B* 26 (1982) 7076.
- [27] K.W. Jacobsen, J.K. Nørskov, *Phys. Rev. Lett.* 65 (1990) 1788.
- [28] F. Jensen, F. Besenbacher, E. Lægsgaard, I. Stensgaard, *Phys. Rev. B* 42 (1990) 9206.
- [29] I.K. Robinson, E. Vlieg, *Phys. Rev. B* 42 (1990) 6954.
- [30] D.J. Coulmann, J. Wintterlin, R.J. Behm, G. Ertl, *Phys. Rev. Lett.* 64 (1990) 1761.
- [31] S.M. Foiles, M.I. Baskes, M.S. Daw, *Phys. Rev. B* 33 (1986) 7983.
- [32] J. Tersoff, R.M. Tromp, *Phys. Rev. Lett.* 70 (1993) 2782.